Total Field and Scattered Field Technique for Fourth-Order Symplectic Finite Difference Time Domain Method *

SHA Wei(沙威), HUANG Zhi-Xiang(黄志祥), WU Xian-Liang(吴先良)**, CHEN Ming-Sheng(陈明生)

Key Laboratory of Intelligent Computing and Signal Processing of Ministry of Education, Anhui University, Hefei 230039

(Received 20 September 2005)

Using symplectic integrator propagator, a three-dimensional fourth-order symplectic finite difference time domain (SFDTD) method is studied, which is of the fourth order in both the time and space domains. The method is nondissipative and can save more memory compared with the traditional FDTD method. The total field and scattered field (TF-SF) technique is derived for the SFDTD method to provide the incident wave source conditions. The bistatic radar cross section (RCS) of a dielectric sphere is computed by using the SFDTD method for the first time. Numerical results suggest that the SFDTD algorithm acquires better stability and accuracy compared with the traditional FDTD method.

PACS: 41. 20. Jb, 02. 40. Yy, 03. 50. De

Symplectic methods include a variety of time discretization methods designed to preserve the global symplectic structure of the phase space for a Hamiltonian system. They show substantial benefits in numerical computation for Hamiltonian systems, especially in long-term simulations. Recently, the symplectic methods have been introduced to computational electromagnetics (CEM). The advantages of the symplectic methods have been verified in Refs. [1–11].

In Ref. [9], we proposed a new method for solving two-dimensional Maxwell's equations employing the symplectic partitioned Runge–Kutta method. In this Letter, we report our further research directly in the three-dimensional (3-D) case. A fourth-order symplectic finite difference time domain (SFDTD) method is derived by using a symplectic integrator propagator, which is of fourth-order in both the time and space domains. The method is nondissipative and can save more memory compared to the traditional FDTD method.[12]

In particular, we mainly deal with the TF-SF technique using the SFDTD method. By revising the SFDTD formulation near TF-SF boundaries, a general sine waves and a gaussian pulse source are successfully propagated in the total field without any leakage to the scattered field region.

Maxwell's equations in a homogeneous, lossless, and sourceless medium can be written in a matrix form as

$$\frac{\partial}{\partial t}\begin{pmatrix}\boldsymbol{H}\\ \boldsymbol{E}\end{pmatrix} = (U+V)\begin{pmatrix}\boldsymbol{H}\\ \boldsymbol{E}\end{pmatrix}, \tag{1}$$

$$U = \begin{pmatrix}\{0\}_{3\times3} & -\mu^{-1}R\\ \{0\}_{3\times3} & \{0\}_{3\times3}\end{pmatrix},$$

$$V = \begin{pmatrix}\{0\}_{3\times3} & \{0\}_{3\times3}\\ \varepsilon^{-1}R & \{0\}_{3\times3}\end{pmatrix}, \tag{2}$$

where R is a 3×3 matrix representing the three-dimensional curl operator, μ and ε is the permittivity and permeability. Equation (1) represents a system of the first-order linear ordinary differential equations that have the following analytical solutions:

$$\begin{pmatrix}\boldsymbol{H}\\ \boldsymbol{E}\end{pmatrix}(\Delta_t) = \exp(\Delta_t(U+V))\begin{pmatrix}\boldsymbol{H}\\ \boldsymbol{E}\end{pmatrix}. \tag{3}$$

Since the matrices U and V do not commute (i.e., $UV \neq VU$), in the time domain the symplectic integrator propagator can be adopted approximately to be

$$\begin{aligned}\exp(\Delta_t(U+V)) &= \prod_{l=1}^{m}\exp(D_l\Delta_t V)\\ &\quad\cdot\exp(C_l\Delta_T U)+O(\Delta_t^{n+1})\\ &= \prod_{l=1}^{m}(I_6+D_l\Delta_t V)(I_6+C_l\Delta_t U)\\ &\quad+O(\Delta_t^{n+1}),\end{aligned} \tag{4}$$

where I_6 is the 6×6 unit matrix , C_l and D_l is the constant coefficients of the propagator obeying symmetry relations $C_l = C_{m+1-l}$ $(0<l<m+1)$, $D_l = D_{m-l}$ $(0<l<m)$ and $D_m = 0$, m is the stage number or iterated number needed in every integer time step, n is the order of approximation. When $m=5$ and $n=4$ are chosen, the fourth-order integrator propagator is obtained. These coefficients can be found in Ref. [4].

In the space domain, we use the fourth-order difference operators to discretize the first-order space differential operators as follows:

$$\left(\frac{\partial f}{\partial x}\right)_i \approx \frac{27(f_{i+1/2}-f_{i-1/2})-f_{i+3/2}+f_{i-3/2}}{24\Delta_x}. \tag{5}$$

Thus the proposed method is referred to as the (4, 4) method. The detailed expressions of the x component of the normalized $\boldsymbol{E}(E_x)$ in the (4, 4) method can be

* Supported partially by the National Natural Science Foundation of China under Grant No. 60371041

** To whom correspondence should be addressed. Email: xlwu@ahu.edu.cn

derived as

$$
\begin{aligned}
E+_x^{n+l/5}\Big(i+\frac{1}{2},j,k\Big) &= E_x^{n+(l-1)/5}\Big(i+\frac{1}{2},j,k\Big) \\
&+ \frac{1}{\varepsilon_r}\Big[Coef_1 \times \Big\{H_z^{n+(l-1)/5}\Big(i+\frac{1}{2},j+\frac{1}{2},k\Big) \\
&- H_z^{n+(l-1)/5}\Big(i+\frac{1}{2},j-\frac{1}{2},k\Big) \\
&- H_y^{n+(l-1)/5}\Big(i+\frac{1}{2},j,k+\frac{1}{2}\Big) \\
&+ H_y^{n_(l-1)/5}\Big(i+\frac{1}{2},j,k-\frac{1}{2}\Big)\Big\} \\
&+ Coef_2 \times \Big\{H_z^{n+(l-1)/5}\Big(i+\frac{1}{2},j+\frac{3}{2},k\Big) \\
&- H_z^{n+(l-1)/5}\Big(i+\frac{1}{2},j-\frac{3}{2},k\Big) \\
&- H_y^{n+(l-1)/5}\Big(i+\frac{1}{2},j,k+\frac{3}{2}\Big) \\
&+ H_y^{n+(l-1)/5}\Big(i+\frac{1}{2},j,k-\frac{3}{2}\Big)\Big\}\Big], \qquad (6)
\end{aligned}
$$

$$
Coef_1 = \frac{9}{8}D_l \times CFL, \quad Coef_2 = \frac{-1}{24}D_l \times CFL, \qquad (7)
$$

$$
CFL = \frac{\Delta_t}{\Delta_s\sqrt{\mu_0\varepsilon_0}}, \qquad (8)
$$

where ε_r is the local relative permittivity at point $(i+1/2,j,k)$ and $\varepsilon = \varepsilon_r\varepsilon_0$, CFL is the Courant–Friedrichs–Levy number, Δ_t and Δ_s are the temporal and uniform spatial increments, respectively.

We consider the plane wave propagating in the y direction and $\boldsymbol{E}$ is polarized in the z direction. We choose a source point k_s, and incident E_z is added at the point. Here the fourth-order discretization for incident field is also used, i.e.

$$
\begin{aligned}
E_{inc,z}^{n+l/5}(j) &= E_{inc,z}^{n+(l-1)/5}(j) \\
&+ Coef_1 \times \Big[H_{inc,x}^{n+(l-1)/5}\Big(j-\frac{1}{2}\Big) \\
&- H_{inc,x}^{n+(l-1)/5}\Big(j+\frac{1}{2}\Big)\Big] \\
&+ Coef_2 \times \Big[H_{inc,x}^{n+(l-1)/5}\Big(j-\frac{3}{2}\Big) \\
&- H_{inc,x}^{n+)l-1)/5}\Big(j+\frac{3}{2}\Big)\Big], \qquad (9)
\end{aligned}
$$

$$
E_{inc,z}^{n+l/5}(k_s) = T[n(l)\Delta_t], \quad n(l) = n + \sum_{m=1}^{l} C_m, \qquad (10)
$$

where T is a time function of the incident wave.

Perfect absorbing boundary conditions (ABCs) defined in Eq. (11) are added at every integer time step, if we set CFL $= 0.5$, then

$$
E_{inc,z}^{n}(1) = E_{inc,z}^{n-2}(2), \quad E_{inc,z}^{n}(0) = E_{inc,z}^{n-2}(1), \qquad (11)
$$

Unlike the traditional FDTD method, we at least apply similar ABCs to three begin points and three endpoints. Generally, in our numerical examples one-dimensional source CFL=0.5 is kept to be unchangeable, but we change it in the three-dimensional case.

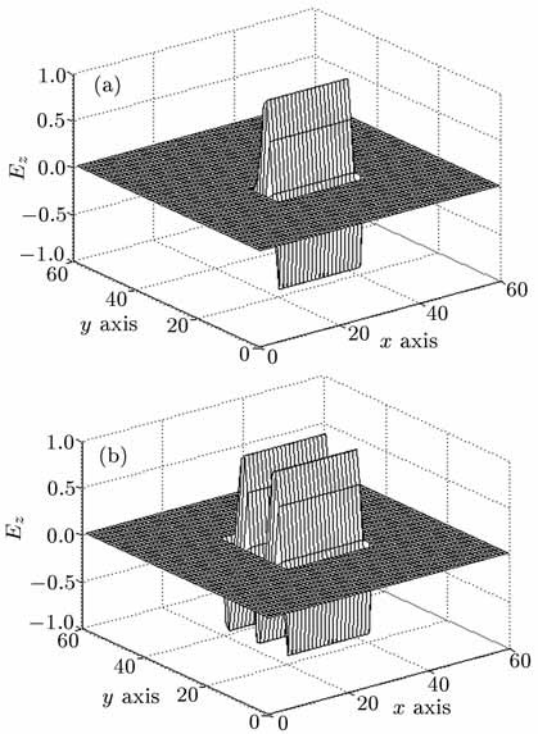

Fig. 1. The snapshot of E_z in the x-y plane at different time step: (a) $n = 20$ and (b) $n = 60$.

We can obtain the source conditions for all fields, if their concrete positions are figured out. The fields must be modified according to the requirements of consistency between the TF-SF boundaries. For example, the consistency conditions for E_z at the TF-SF boundary $j = j_0$ grid plane are given as follows:

$$
\begin{aligned}
E_z^{n+l/5}\Big(i,j_0-1,k+\frac{1}{2}\Big) &= E_z^{n+l/5}\Big(i,j_0-1,k+\frac{1}{2}\Big) \\
&+ Coef_2 \times H_{inc,x}^{n+l/5}\Big(j_0+\frac{1}{2}\Big), \qquad (12)
\end{aligned}
$$

$$
\begin{aligned}
E_z^{n+l/5}\Big(i,j_0,k+\frac{1}{2}\Big) &= E_z^{n+l/5}\Big(i,j_0,k+\frac{1}{2}\Big) \\
&+ Coef_1 \times H_{inc,x}^{n+l/5}\Big(j_0-\frac{1}{2}\Big) \\
&+ Coef_2 \times H_{inc,x}^{n+l/5}\Big(j_0=\frac{3}{2}\Big), \qquad (13)
\end{aligned}
$$

$$
\begin{aligned}
E_z^{n+l/5}\Big(i,j_0+1,k+\frac{1}{2}\Big) &= E_z^{n+l/5}\Big(i,j_0+1,k+\frac{1}{2}\Big) \\
&+ Coef_2 \times H_{inc,x}^{n+l/5}\Big(j_0-\frac{1}{2}\Big). \qquad (14)
\end{aligned}
$$

A gaussian pulse plane wave with $E_{inc,z} = \exp[-(n-10)^2/50]$ propagating along the y direction is considered. The snapshot of E_z in the $x-y$ plane at different time steps is shown in Fig. 1. We discretize the problem using a cube grid. The simulation domain is $60 \times 60 \times 60$ cells, and the total field (TF) contains $20 \times 20 \times 20$ cells. The source point is set at the fifth grid away from the boundary of the TF region. We choose $\Delta_s = 0.1$ with being wavelength and set three-dimensional CFL=0.5. When $n = 20$, the wave just enters into the TF region. When $n = 60$, half the wave packet has moved out of the TF region.

Meanwhile, the largest magnitude of the field value in the SF zone is lower than the order of 10^{-10}.

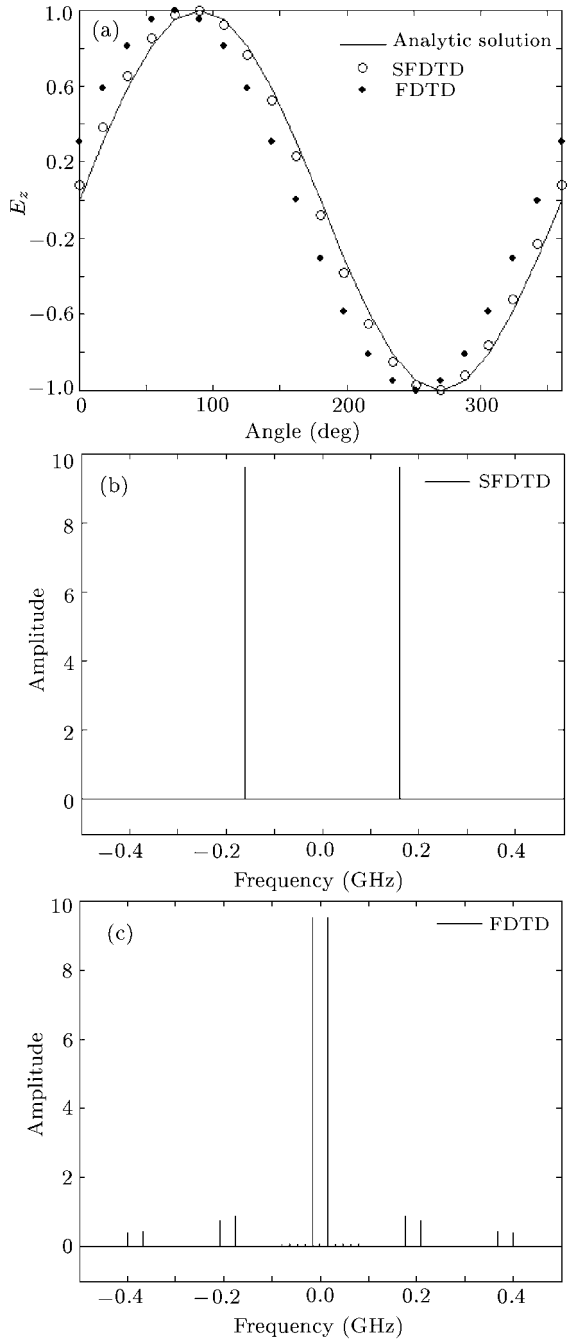

Fig. 2. A three-dimensional sine plane wave E_z at the same point within one period: (a) Time-domain profile waveform, and amplitude spectra of the profile waveform (b) in the SFDTD scheme and (c) in the FDTD method.

Next we set 3-D CFL=1.0, $\Delta_s = 0.1$ wavelength. We draw one-dimensional projection of 3-D sine plane wave at the same point within one period in Fig. 2. In addition, amplitude spectrum is calculated by fast Fourier transform. From Fig. 2(b), using the SFDTD method, the electric field profile propagates without any changes in the profile compared with the analytic solution. While in Fig. 2(c), the results clearly show that the SFDTD method acquires better accuracy and numerical dispersion than traditional FDTD method under the same stability condition.

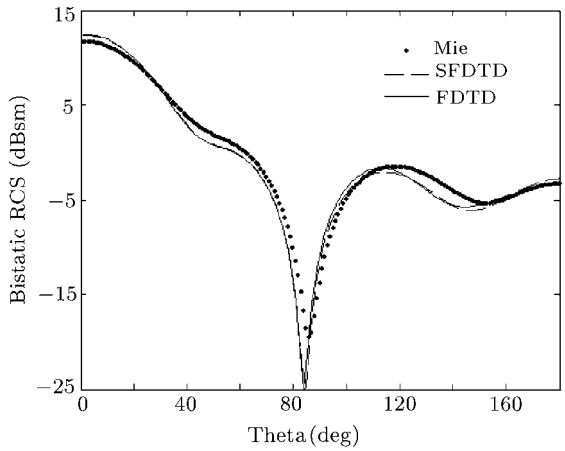

Fig. 3. ***E***-plane bistatic RCS of the dielectric sphere.

Finally, we consider a dielectric sphere illuminated by a plane wave propagating in the z direction and $\boldsymbol{E}$ polarized in the x direction. The frequency of the incident wave is 300 MHz. The sphere has a diameter of 1.0 m, a relative permittivity $\varepsilon_r = 4.0$, and a conductivity of 0.3. The size of the cell is 0.05 m and CFL is 0.5. The total computational domain is $83 \times 83 \times 83$ cells, total field occupies $68 \times 68 \times 68$ cells. The bistatic RCS in the $\boldsymbol{E}$-plane is simulated within 1700 time steps. Mie series is presented as the reference solution. From Fig. 3, the results obtained by the SFDTD scheme are better in agreement with the Mie series than the traditional FDTD method. The global relative rms RCS error is obtained to be 0.2147 by using the SFDTD scheme, which is better than 0.2247 of the traditional FDTD method.

References

[1] Hirono T, Lui W and Yokoyama K 1997 *IEEE Microwave Guided Wave Lett.* **7** 279
[2] Hirono T et al 1998 *J. Lightwave Technol.* **16** 1915
[3] Hirono T, Lui W and Seki S 1999 *IEEE MTT-S Int. Microwave Symp. Dig.* (CA: Anaheim) p 1293
[4] Hirono T, Lui W, Seki S and Yoshikuni Y 2001 *IEEE Trans. Microwave Theory Technol.* **49** 1640
[5] Saitoh I, Suzuki Y and Takahashi N 2001 *IEEE Trans. Magn.* **37** 3251
[6] Saitoh I and Takahashi N 2002 *IEEE Trans. Magn.* **38** 665
[7] Li K et al 2003 *Chin. Phys. Lett.* **20** 321
[8] Rieben R, White D and Rodrigue G 2004 *IEEE Trans. Antennas Propagat.* **52** 2190
[9] Huang Z X and Wu X L 2005 *Int. J. Quantum Chem.* (accepted)
[10] Zhai P W et al 2005 *Appl. Opt.* **44** 1650
[11] Chen J B 2004 *Chin. Phys. Lett.* **21** 37
[12] Karl S K and Raymond J L 1993 *The Finite Difference Time Domain Method for Electromagnetics* (Boca Raton, FL: CRC Press)